

On the order of the phase transition in the spin-1 Baxter-Wu model

L. N. Jorge,¹ L. S. Ferreira,² and A. A. Caparica²

¹*Instituto Federal do Mato Grosso - Campus Cáceres,
Av. dos Ramires s/n, 78200-000, Cáceres, MT, Brazil*

²*Universidade Federal de Goiás, Av. Esperança s/n, 74.690-900, Goiânia, GO, Brazil*

In this work we investigate the order of the phase transition of the spin-1 Baxter-Wu model. We used extensive entropic simulations to describe the behavior of quantities which reveal the order of the phase transition. We applied finite-sizing scaling laws for continuous and discontinuous phase transitions. Our results show that this system exhibits an indeterminacy regarding the order of the phase transition, i.e., the results are conclusive for both transitions, whether continuous or discontinuous. In such a scenario we carried out a study of the configurations in the region of the phase transition, which confirmed that the model seems to undergo a tetracritical transition, with the coexistence of a ferromagnetic and three ferrimagnetic configurations, suggesting that it may be a multicritical point belonging to a critical line of an external or a crystalline fields, where the continuous and the discontinuous phase transitions may coexist reflecting different features of the system.

I. INTRODUCTION

The order-disorder transitions in two-dimensional systems have been studied experimentally in structures constituted by adsorbed atoms or molecules in single crystals and their universality class has been experimentally determined. Among them there are some real systems with triplet interactions which belong to the same universality class of the $q = 4$ Potts model. Examples of such compounds are the chemisorbed overlayer $p(2 \times 2)$ oxygen on Ni(111)[1], the adsorption system O/Ru(0001)[2] at $1/4$ monolayer and the (2×2) - $2H$ structure on Ni(111) [3]. They are well-described by a model that considers three spin interactions in a triangular lattice.

In 1972 D. W. Woods and H. P. Griffiths[4] proposed such a model: the Baxter-Wu model(BW). They propounded a system of spins defined in a two-dimensional triangular lattice, with the spins located at the vertices of the triangles, and assuming the integer values ± 1 . An interesting feature of this spin system is that it exhibits an order-disorder transition, but it is not symmetric by inversion of all spins. This model, known as the spin-1/2 case, was exactly solved by R.J. Baxter and F.Y. Wu [5–7] yielding the same critical temperature of the Ising model on a square lattice $k_B T_c / J = 2 / \ln(1 + \sqrt{2}) = 2.2691853\dots$, and critical exponents belonging to the $q = 4$ Potts model universality class, namely $\alpha = \nu = 2/3$, $\beta = 1/12$, and $\gamma = 7/6$. Simulations using the short-time scaling formalism corroborate the exact results for ν and β [8], although not within the error bars. The same occurs in entropic simulations of the $q = 4$ Potts model[9].

This behavior of the BW model should be expected, since both models have the same symmetry and degree of degeneracy in the ground state. However, unlike the BW model, the $q = 4$ Potts model demands logarithmic corrections. Thereby, to investigate this apparent contradiction, Kinzel *et al* [10] studied a generalization of the BW model by insertion of annealed vacancies. In

this new scenario we have the spin-1 Baxter-Wu model where the spins variables can assume one of three discrete values 0 and ± 1 . They found out through the behavior of the correlation length and by using finite size scaling techniques, that a second order transition would happen only for the pure BW model.

Notwithstanding, another study of the spin-1 BW model was carried out by Costa and Plascak[11], using Monte Carlo simulations with the standard Metropolis algorithm. Applying finite size scaling considerations they obtained a critical behavior different from the first work, with a second order transition and well defined critical exponents.

In view of these conflicting results, our expectation in carrying out a detailed study of the model was to detect a pure discontinuous behavior, as predicted by Kinzel or a continuous behavior, as obtained by Costa and Plascak. Nevertheless our findings show that it exhibits a mixed behavior, typical of multicritical points.

A multicritical transition occurs in a region of the phase diagram where multiple phases co-exist. In general, multicritical states emerge in the intersection of a first order and a second order transitions. In such regions it is common the superposition of both transitions[12–17]. Musial [18] applied the Monte Carlo method to the 3D Ashkin-Teller model in the region of the three-critical point and found out an indeterminacy regarding the order of transition of the system. Critical exponents point out to a continuous transition, while the Binder cumulant of energy evidences a discontinuous transition. Another characteristic observed near the tricritical point is the presence of a non-zero valley in the energy probability[19, 20]. In a recent work Dias *et. al.*[21] carried out a study of the spin-1 Baxter-Wu model with a crystalline field and detected the existence of a pentacritical point with the coexistence of three ferrimagnetic and a ferromagnetic configurations, along with that with spins zero.

In the present work we are interested in the characteristics of the order of the phase transition in the spin-1

Baxter-Wu model. Here we employ entropic sampling simulations to construct the density of states, which is estimated for systems with non-multiple of three lattice sizes, following the same implementation of [22]. Some quantities which reveal the order of the transition, as the total magnetization, the energy, and the susceptibility are investigated.

This paper is organized as follows: Section II presents the BW model. In Sec. III we provide details of our simulations. The finite size scaling analysis is showed in section IV. The results are discussed in section V, and in section VI a summary and outlooks are given.

II. THE BAXTER-WU MODEL

In the Baxter-Wu model the three spin interaction is governed by the Hamiltonian

$$H_{BW} = -J \sum_{\langle i,j,k \rangle} s_i s_j s_k, \quad (1)$$

where the spin variables are located at the vertices of the lattice and take on the values $s_i = \pm 1, 0$, J plays the role of a coupling constant that fixes the energy scale, and the sum extends over all triangular faces of the lattice.

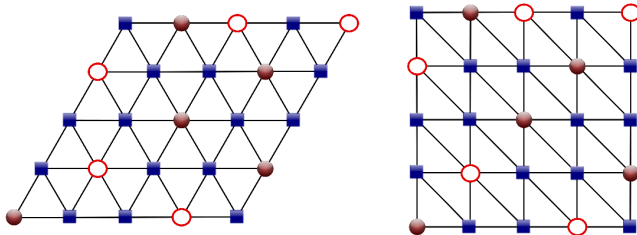


FIG. 1. (color online). Left: Representation of a possible configuration of the Baxter-Wu model as a superposition of three sub-lattices on a triangular lattice. Right: Transposition of the triangular lattice to a square lattice. The cycles represent spins $+1$, the squares spins -1 , and the open cycles the zeros.

In our work we deal with the system by transposing the triangular lattice to a square one, as shown in the right side of Fig.1. One can see that each spin $\sigma_i \equiv s_{i,j}$ has six triangular faces around it, and, if one visits all spins of the configuration computing the six triangular faces for each spin, each triangular face will be counted three times. Thus, the energy of a particular configuration of lattice size L defined by the Hamiltonian (1) can be calculated in the square lattice as

$$E = \frac{J}{3} \sum_{i=1}^L \sum_{j=1}^L s_{i,j} (s_{i-1,j} s_{i,j-1} + s_{i,j-1} s_{i+1,j-1} + s_{i+1,j-1} s_{i+1,j} + s_{i+1,j} s_{i,j+1} + s_{i,j+1} s_{i-1,j+1} + s_{i-1,j+1} s_{i-1,j}). \quad (2)$$

Likewise the $q = 4$ Potts model and the spin-1/2 BW model, in this model, if one assumes multiple of three lattices, four distinct ground states are present, one with all spins positive, giving a ferromagnetic configuration, and other three, where one sublattice remains positive while the other two are negated, yielding ferrimagnetic configurations successively. However, if we choose non-multiple of three lattices, only the ferromagnetic configuration will be present in the ground state and we can choose the order parameter of the system as the sum of all spins of the lattice

$$M = \sum_{i,j=1}^L s_{i,j}. \quad (3)$$

As shown in Ref. [22] the use of multiple or non-multiple of three lattices does not change the results for the critical exponents, such that in the present study we adopted non-multiple of three lattices and the sum over all spins as the order parameter. In order to investigate the order of the phase transition of the model we performed entropic sampling simulations either treating the transition as discontinuous, either as continuous.

III. FINITE SIZE SCALING

A. Continuous phase transition

From the fluctuations in the energy and the magnetization we can calculate the specific heat and the magnetic susceptibility

$$C(T) = (\langle E^2 \rangle - \langle E \rangle^2) / T^2, \quad (4)$$

$$\chi(T) = (\langle m^2 \rangle - \langle m \rangle^2) / T, \quad (5)$$

where E is the energy, m is the magnetization per site and T is the absolute temperature.

Using the free energy definition and the appropriate derivatives of the free-energy density one can obtain scaling relations for various thermodynamic quantities[23, 24], such as

$$m_L(t) \approx L^{-\beta/\nu} \mathcal{M}(tL^{1/\nu}), \quad (6)$$

$$\chi_L(t) \approx L^{\gamma/\nu} \mathcal{X}(L^{1/\nu} t), \quad (7)$$

$$c_L(t) \approx L^{\alpha/\nu} \mathcal{C}(tL^{1/\nu}), \quad (8)$$

where L is the linear size of the lattice, $t = (T_c - T)/T$ is the reduced temperature and α , β , γ and ν are the static critical exponents that obey the scaling relation

$$2 - \alpha = d\nu = 2\beta + \gamma, \quad (9)$$

where d is the dimensionality of the system. As $L \rightarrow \infty$, the pseudocritical temperature of the finite lattice obeys the scaling law

$$T_L = T_c + \lambda L^{-1/\nu} \quad (10)$$

where λ is a constant, T_c is the critical temperature of the infinite system, and T_L is the effective transition temperature for the lattice of linear size L .

One can obtain the critical exponent ν using the logarithmic derivatives of the magnetization [25, 26].

$$[m^n] \equiv \ln \frac{\partial \langle m^n \rangle}{\partial T}, \quad (11)$$

which have the same scaling behavior of the 4th order Binder cumulant. Following the prescriptions of the works [22, 26], we use the set of thermodynamic quantities that are functions of the logarithmic derivatives of the magnetization

$$V_1 \equiv 4[m^3] - 3[m^4], \quad (12)$$

$$V_2 \equiv 2[m^2] - [m^4], \quad (13)$$

$$V_3 \equiv 3[m^2] - 2[m^3], \quad (14)$$

$$V_4 \equiv (4[m] - [m^4])/3, \quad (15)$$

$$V_5 \equiv (3[m] - [m^3])/2, \quad (16)$$

$$V_6 \equiv 2[m] - [m^2]. \quad (17)$$

Using Eq. (6) it is immediate to show that

$$V_j \approx \frac{1}{\nu} \ln L + \mathcal{V}_j(tL^{\frac{1}{\nu}}), \quad (18)$$

for $j = 1, 2, \dots, 6$. At the critical temperature $T_c(t = 0)$ the \mathcal{V}_j are constants independent of the lattice size L , therefore we can estimate $1/\nu$ by the slopes of V_j calculated at T_L . With the exponent ν already obtained, the next step is calculating the critical temperature using Eq. 10 and the exponents β and γ from the slopes of the log-log plot of Eqs. 6 and 7 at the critical temperature T_c . A model with continuous phase transition displays well defined critical exponents and allows the determination of the critical temperature by the scaling relation of Eq. (10).

B. Discontinuous phase transition

In a discontinuous phase transition the scaling relations defined in the continuous transition do not hold.

Usually the thermodynamic properties, such as magnetization and specific heat scale with the system dimension. The critical temperature of the system may be determined using the cumulant of the energy that scales with the lattice size [27]. The fourth order cumulant of the energy is defined as

$$U_E(T) \equiv 1 - \frac{\langle E^4 \rangle_T}{3\langle E^2 \rangle_T^2}. \quad (19)$$

This function has a minimum [28–30], which temperature scales as

$$T_L = T_c + \lambda L^{-d}. \quad (20)$$

where d is the dimension of the system. Extrapolation for $L \rightarrow \infty$ gives the critical temperature T_c for the infinite system.

The behavior of the cumulant of the magnetization, given by

$$U_M(T) \equiv 1 - \frac{\langle M^4 \rangle_T}{3\langle M^2 \rangle_T^2}. \quad (21)$$

also may suggest a discontinuous phase transition. In this case we have the presence of a sharp minimum and the crossing of the curves of different lattice sizes taking place around the critical temperature [27, 31].

Another way of finding the critical temperature is the analysis of the peaks of the energy probability. In the region of the critical temperature this probability should have a double peak of same height and the region between the peaks should have a null probability [31–33]. In the canonical ensemble the energy probability is calculated as

$$P(E, T) = g(E) e^{-\frac{E}{k_B T}}. \quad (22)$$

This method allows calculating the latent heat of the transition as the energy difference ΔE_L between the two peaks, which obeys the scaling relation of L^{-1} [31]. The temperatures where the peaks reach the same height also scales as Eq. 20.

If the entropy is given as a function of the energy one can calculate the microcanonical temperature directly by the definition

$$\beta = \frac{1}{T} = \frac{\partial S}{\partial E}, \quad (23)$$

and the behavior of this quantity changes with the order of the phase transition. In the discontinuous transition it has a s -like shape and a straight line at the critical temperature divides it into two areas of same size [34, 35].

IV. ENTROPIC SIMULATIONS

Our computational approach follows the Wang-Landau method [36, 37], except that we include some improvements proposed in [38–41], which are: i) the density of

states is not updated at every spin flip, but, only after each Monte Carlo sweep, in order to pick uncorrelated configurations when we construct the density of states; ii) to avoid unnecessary extensive simulations, we perform them until $\ln f = \ln f_{final}$, defined by the canonical averages along the simulation. In [38] a checking parameter ε was proposed. It signals automatically when the simulations should be halted. One consequence of adopting the checking parameter is that f_{final} may be different for different runs; and, iii) at the beginning of the simulations, the microcanonical averages should not be accumulated before $\ln f = \ln f_{micro}$ (also defined by canonical averages during simulations), since, at the beginning of the simulations the configurations do not match those to maximum entropy. These three adjustments provide more accurate results, save CPU time and have the advantage of being easily implementable.

Once the density of states is constructed, one can calculate the canonical average of any thermodynamic quantity X as

$$\langle X \rangle_T = \frac{\sum_E \langle X \rangle_E g(E) e^{-\beta E}}{\sum_E g(E) e^{-\beta E}}, \quad (24)$$

where $\langle X \rangle_E$ is the microcanonical average accumulated along the simulations, $\beta = 1/k_B T$, where T is the absolute temperature given in units of J/k_B and k_B is the Boltzman's constant.

In Ref.[38] it was also noted that two independent similar finite-size scaling procedures can lead to very different results for the critical temperature and exponents, which often do not agree within the error bars. To overcome this difficulty we carry out 10 independent sets of finite-size scaling procedures. The final results for the critical exponents and critical temperature are obtained as an average over all sets.

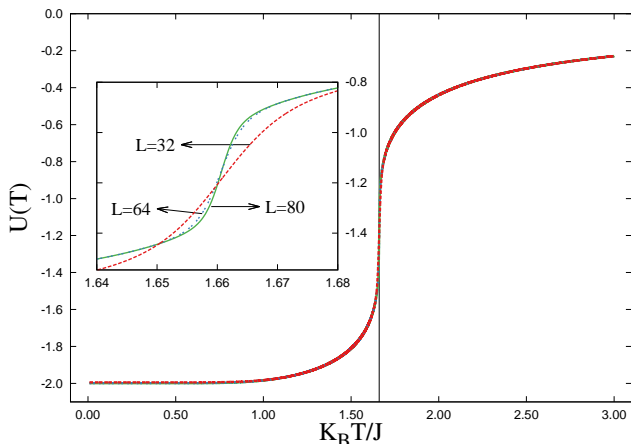


FIG. 2. Mean Energy.

V. RESULTS

We study the spin-1 BW model on a square lattice with $N = L \times L$ sites, by performing the entropic simulations described above. We perform ten studies of finite size scaling using the following lattice sizes : $L = 32, 40, 44, 52, 56, 64, 76, 80, 86,$ and 92 , with $N = 24, 20, 20, 16, 16, 12, 12, 12,$ and 12 runs for each size, respectively. The choice of these lattice sizes was based in the work of Jorge *et al* [22], where it was shown that one can simulate the BW model using non-multiple of three lattices and obtain the same results of the multiple of three ones.

Before presenting the results for continuous and discontinuous phase transitions, we analyze the behavior of energy, magnetization, specific heat, and magnetic susceptibility. Figs. 2 and 3 show the energy and the magnetization as functions of temperature for $L = 32, 64,$ and 80 . The main graphs suggest a discontinuous phase transition with an abrupt variation in the region of the critical temperature. But if we look at the zoom in the insets in a narrow range of temperature, we observe a more likely continuous behavior.

For the specific heat and magnetic susceptibility, shown in Figs 4 and 5, we see that the peaks are around very close temperatures for all the lattice sizes so that a finite size scaling behavior is not visible to the eyes. In fact the finite size scaling effects for the critical temperature are very subtle when one uses non multiple of three lattices in the BW model[22]. All these observations are therefore not conclusive about the order of the phase transition.

A. Continuous phase transition

In order to investigate if the system undergoes a continuous phase transition we carried out a study seeking out for critical exponents and critical temperature. By locating the maxima of the relations defined in Eqs. (12)-

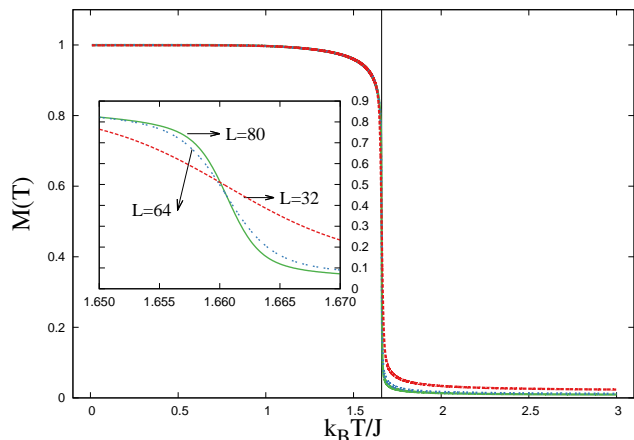


FIG. 3. Magnetization.

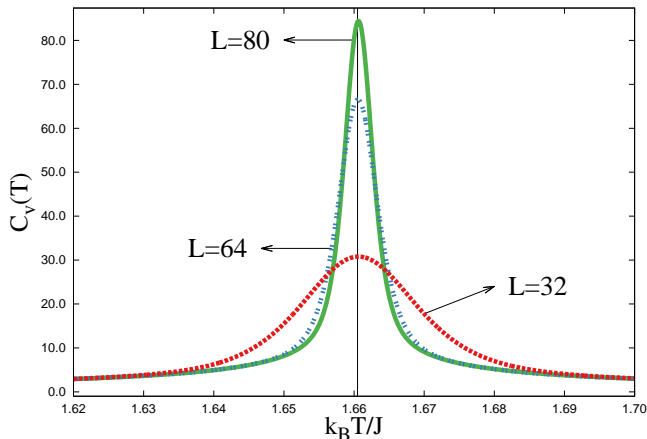


FIG. 4. Specific Heat of lattice sizes non multiple of three.

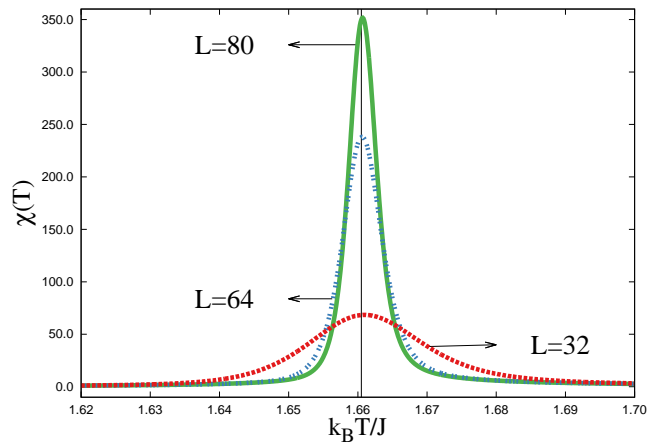


FIG. 5. Susceptibility of lattice sizes non multiple of three.

(17), which scales as shown in Eq. (18), we find $1/\nu$ as the slopes of the straight lines of the plots of V_j against $\ln L$, since in $T_c(t=0)$ the coefficients \mathcal{V}_j are constants independent of the lattice size L .

Fig.6 shows the six slopes, where for each one of them was calculated $\nu = 1 / (\frac{1}{\nu})$ with error $\Delta\nu = \Delta(\frac{1}{\nu}) / (\frac{1}{\nu})^2$. The graph presents only one of the ten sets of the performed finite size scaling simulations.

The value obtained on each set is shown in the first column of Table I and the final result $\nu = 0.6438(10)$ appears in the last line.

With the exponent ν accurately determined we proceed to estimate the critical temperature and the exponents β and γ . In Fig. 7 we use Eq. (10) to determine T_c as the extrapolation to $L \rightarrow \infty$ ($L^{-1/\nu} = 0$) of the linear fits given by the locations of the maxima of the specific heat and the magnetic susceptibility. As expected the points look badly aligned because of the proximity of the points to the exact value. In Fig. 8 we depict the log-log plot of the magnetization at the critical temperature calculated by Eq. (6). The slope

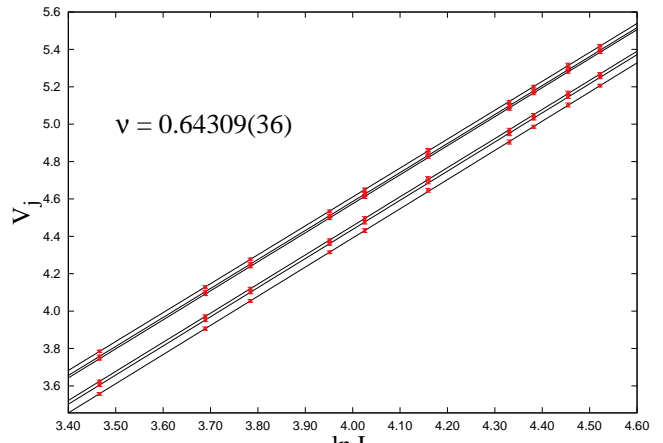


FIG. 6. Size dependence of V_j at the critical temperature. The slopes yield $1/\nu$.

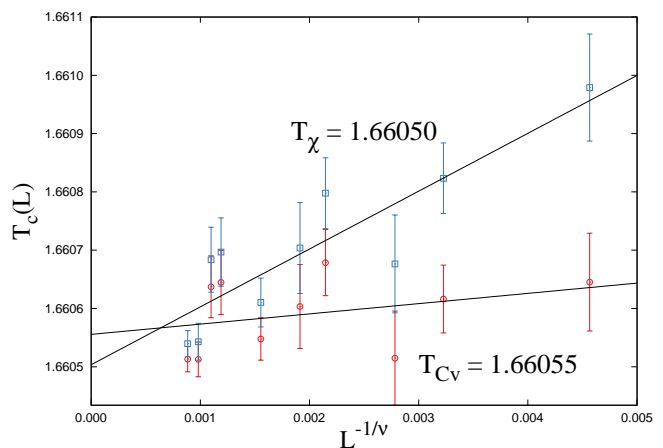


FIG. 7. Size dependence of the locations of the extrema in the specific heat and the magnetic susceptibility with $\nu = 0.6438$.

gives β/ν , so that we obtain $\beta = \nu \frac{\beta}{\nu}$, with the error $\Delta\beta = \frac{\beta}{\nu} \Delta\nu + \nu \Delta \frac{\beta}{\nu}$, yielding $\beta = 0.0896(69)$. Fig. 9 displays the log-log plot of the maxima of the susceptibility, where we obtain $\gamma = 1.1629(42)$. In the last three columns of Table I we present the results for all the 10 sets for β , γ , and T_c , with the final mean values $\beta = 0.0762(75)$, $\gamma = 1.1611(28)$, and $T_c = 1.660549(51)$ in the last line. These results with well defined critical exponents and critical temperature point out to a typical continuous phase transition corroborating the conclusions of Costa and Plascak[11].

B. Discontinuous phase transition

Considering the system as undergoing a discontinuous phase transition we analyze the behavior of the fourth-order Binder energy and magnetization cumulants, and the energy probability distribution. In Fig. 10 we show

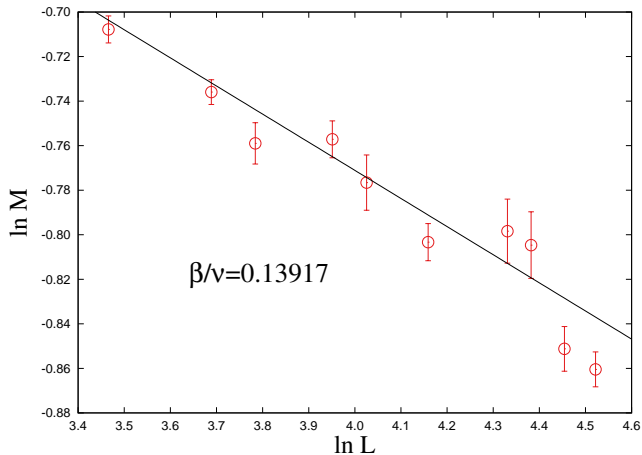


FIG. 8. Log-log plot of size dependence of the magnetization at $T_c = 1.660549$.

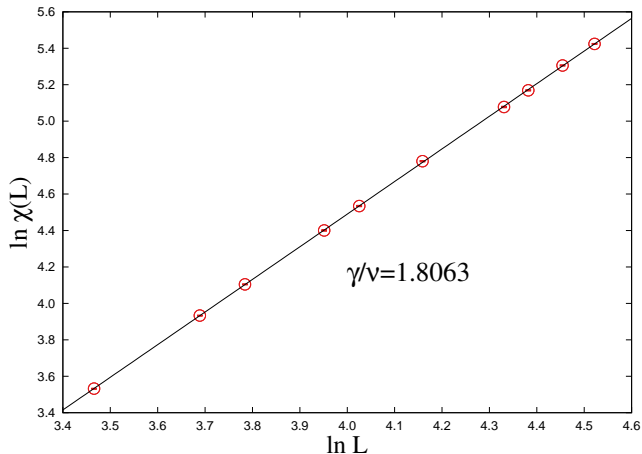


FIG. 9. Log-log plot of size dependence of the maxima of the susceptibility.

TABLE I. Ten finite size scaling results for the critical temperature, T_c , and the exponents ν , β and γ . The averages over all runs are shown in the last line.

ν	β	γ	T_c
0.64309(36)	0.0896(69)	1.1629(42)	1.660469(26)
0.64309(47)	0.0854(82)	1.1640(52)	1.660480(34)
0.64568(22)	0.0760(56)	1.1588(42)	1.660556(25)
0.64404(33)	0.0722(74)	1.1576(48)	1.660568(32)
0.64365(32)	0.0663(35)	1.1622(42)	1.660607(15)
0.64463(42)	0.0667(54)	1.1594(56)	1.660624(21)
0.64442(39)	0.0734(58)	1.1584(45)	1.660575(24)
0.64373(35)	0.0761(54)	1.1610(45)	1.660556(23)
0.64413(32)	0.0815(78)	1.1604(42)	1.660504(29)
0.64178(37)	0.0753(78)	1.1663(44)	1.660552(33)
0.6438(10)	0.0762(75)	1.1611(28)	1.660549(51)

the energy cumulant for three lattice sizes $L = 32, 64$, e 80 . One can see that the curves present a minimum

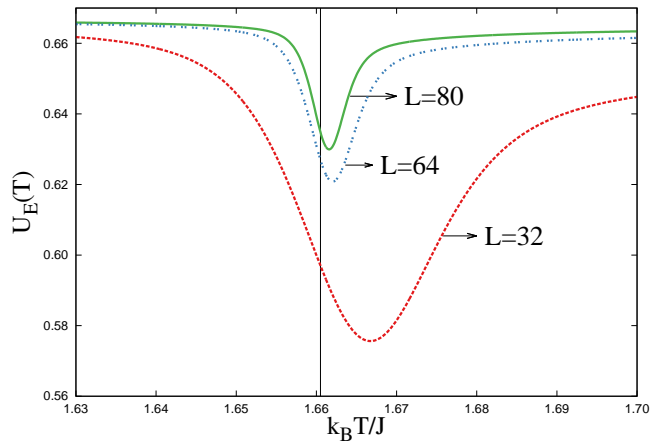


FIG. 10. Behavior of the cumulant of energy. The vertical line demarcates the critical temperature estimated using scaling laws for the continuous transition

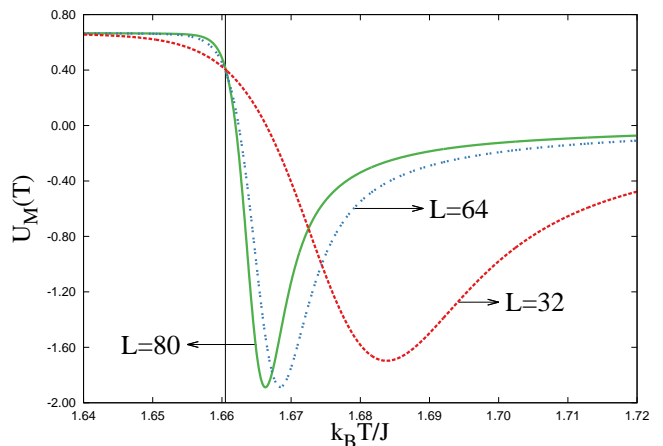


FIG. 11. Behavior of the cumulant of magnetization. The vertical line demarcates the critical temperature estimated using scaling laws for the continuous transition

in the region of the critical temperature and the temperatures of these extrema approach the critical temperature, while the values of the functions tend to something around 0.666.

For the magnetization cumulant we have a typical discontinuous transition behavior characterized by a prominent minimum and the crossing of the cumulants of different sizes at the critical temperature, as shown in Fig. 11 where we depict the cumulant of magnetization for $L = 32, 64$, e 80 . The vertical line in Figs. 10 and 11 demarcates the critical temperature estimated using scaling laws for the continuous transition.

In Fig. 12 we present two other quantities, which characterize a discontinuous transition behavior: the energy probability and the inverse microcanonical temperature. In the top we show the energy probability as a function of the energy per particle for three lattice sizes.

At the transition temperature we observe a double

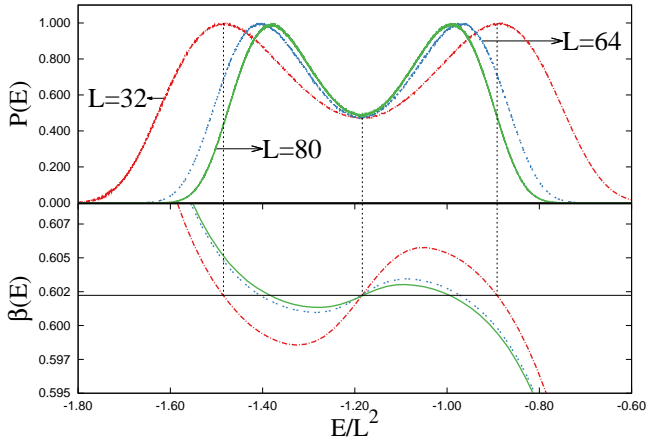


FIG. 12. (Top) Canonical distribution of $P(E)$. (Bottom) Microcanonical inverse temperature. The horizontal line demarcates the critical temperature estimated using scaling laws for the continuous transition.

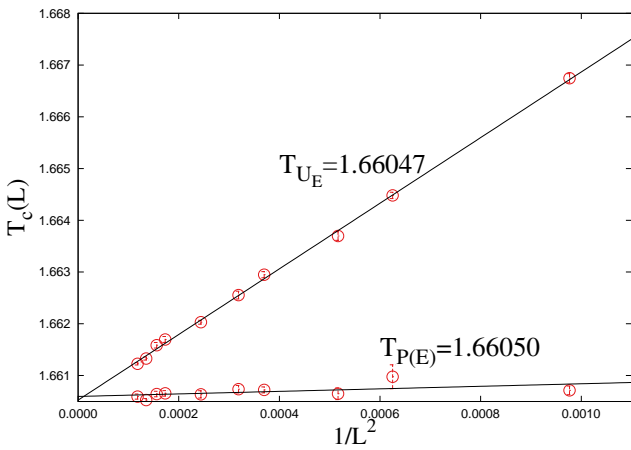


FIG. 13. Fitting of the temperatures of the minima of the cumulant of energy and of the temperatures where the same height in $P(E)$ occurs, determining the critical temperature.

peak of same height and a valley between them with non-zero probability. In the bottom we display the microcanonical inverse temperature as a function of energy revealing a manifest discontinuous transition behavior. The horizontal line represents the critical temperature obtained by means of scaling laws for a continuous transition. One can see that the crossing of the curves occurs around the critical temperature and that the minimum of the probability in the valley coincides with this point.

Using the scaling laws for the minimum of the energy cumulant and the energy probability Eq. 20, we can estimate the critical temperature of the system. The linear fitting of these two quantities are represented in Fig. 13. These are the results of the first of ten sets of samplings. One can see that the values agree with those obtained by means of the analysis of a continuous transition using

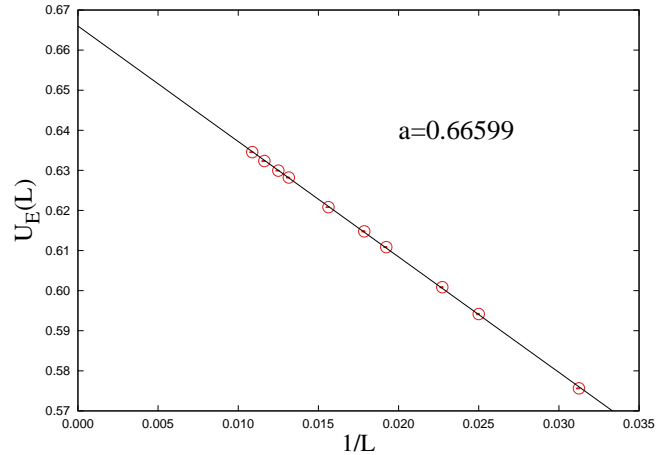


FIG. 14. Linear fitting of the minimum of the cumulant of energy with $1/L$.

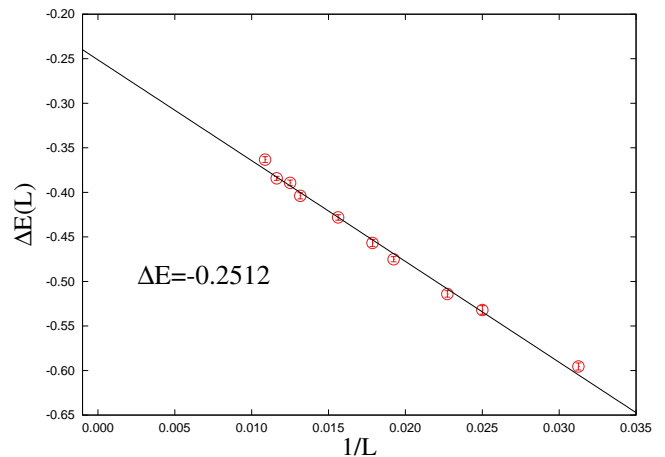


FIG. 15. Variation of the energy between the peaks of the energy probability against $1/L$.

the specific heat and the susceptibility.

Two other additional results that corroborate the discontinuous phase transition are the linear fitting of the minimum of the energy cumulant, which converges to 0.666... for an infinite system, and the fitting of the variation of the energy between the peaks of the energy probability, the latent heat. We present these two quantities in Figs. 14 and 15, respectively. In both situations one can see a typical discontinuous transition behavior.

In Fig. 14 we show the fitting of the minimum of the energy cumulant as a function of $1/L$ using $U_E(L, T_c) = a + bL^{-1}$. We see that $\lim_{L \rightarrow \infty} U_E(L, T_c) = 2/3$ as expected [31]. In its turn Fig. 15 displays the fitting of the variation of energy between the peaks of the energy probability at the critical temperature as a function of $1/L$. We see that as $L \rightarrow \infty$ the peaks keep an energy difference of $|\Delta E| = 0.2512$, which reveals the existence of a latent heat, which is characteristic of a discontinuous

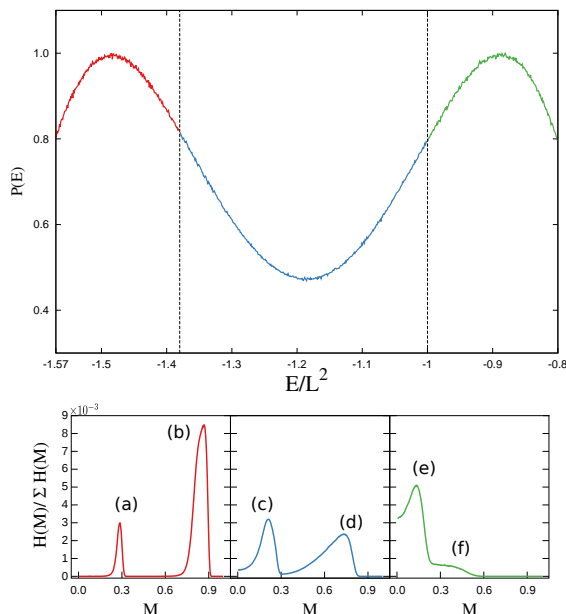


FIG. 16. (Top) Canonical Distribution of $P(E)$ at the temperature of same height. (Bottom) Histograms of the magnetization in the regions close to the peaks and the valley.

transition.

C. Coexistence of continuous and discontinuous phase transitions

So far we have analyzed the system adopting two different approaches: i) considering that it undergoes a continuous phase transition, and ii) the phase transition is discontinuous. In the first case we have obtained quantities typical of this transition, such as the critical exponents $\nu = 0.6438(10)$, $\beta = 0.0762(75)$ and $\gamma = 1.1611(28)$, and the critical temperature $T_c = 1.660549(51)$, as prescribed by [11], confirming therefore that the system undergoes a continuous phase transition. It is also worthwhile to note that these results are very close to the exact solution for the BW spin 1/2: $\nu \cong 0.6667$, $\beta \cong 0.0833$, and $\gamma \cong 1.1667$. On the other hand, assuming that the transition is discontinuous, the system behaves this way, with a critical temperature $T_c = 1.66055(38)$, and a latent heat $|\Delta E| = 0.2512$, as described by Kinzel [10]. We are thus faced with an indeterminacy, which is characteristic of a multicritical transition. In such situation the question is: which are the phases present in the criticality?

In order to address this discussion we have to analyze the configurations that appear at the criticality. First we have to define an interval of more probable energies at the critical temperature. The energy probability at the critical temperature $P(E) = g(E)e^{-E/k_B T_c}$ displays two peaks revealing the two more probable energies, and a non-null valley between them. We can therefore define three energy intervals: one around the lower energy

peak, a second between the peaks, and the last close to the highest energy peak, as shown in top of Fig. 16 for $L = 32$. For each of these regions we constructed histograms of the magnetization, which are shown in bottom of Fig. 16. In all cases we observe the presence of two peaks. The peak (a) is related to ferrimagnetic configurations with magnetization around $-L^2/3$, while the peak (b) correspond to ferromagnetic configurations with magnetization close to L^2 , as shown in Fig. 17 (a) and (b). The black, white and gray squares represent the spins $+1$, -1 e 0 , respectively. We see that in Fig. 17(a) we have the predominance of the ferrimagnetic configuration with some spins 0 points and the occurrence of some paramagnetic blocks, and in Fig. 17(b) the predominance of the ferromagnetic configuration, with some points of spins 0 and the occurrence a few paramagnetic blocks. In its turn the peaks (c) and (d) of Fig. 16 correspond to configurations with the predominance of ferri- and ferromagnetic agglomerates, respectively, with the presence of spins 0, some islands diverse of the predominant, and small paramagnetic blocks, as observed in Fig. 17 (c) and (d). Its worthwhile mentioning that in (d) there is a higher incidence of paramagnetic clusters then in (c). In peaks (e) and (f) we see that the system is closer to disorder, but there is still a noticeable presence of ferrimagnetic and ferromagnetic clusters in each of them, respectively.

It is important to notice that each ferrimagnetic cluster, as in Fig. 17 (a) can belong to one of the three possible ground state ferrimagnetic configurations, in such a way that all the situations described above correspond to the coexistence of three ferrimagnetic and a ferromagnetic configurations, along with the paramagnetic configuration indicating that we are dealing with a tetracritical order-disorder transition, since all these configurations coexist at the critical temperature. All these evidences, such as the indeterminacy of the order of the phase transition and the non-null valley in the energy probability, point out to the behavior of a tetracritical point, which can correspond to the zero field state of critical lines of external or crystalline fields.

All the discussion above led to a non-conclusive result on the order of the phase transition of the spin-1 Baxter Wu model, suggesting a coexistence of the continuous and the discontinuous phase transitions. It seems quite controversial, but a recent publication[42] shows the coexistence of first and second order electronic phase transition in a correlated oxide, where the sample bulk exhibits a first-order transition between metal and insulator phases, while the anomalous nanoscale domain walls in the insulating state undergo a distinctly continuous insulator-metal transition, with characteristics of second-order behavior. Such example encourage us to suggest that the ferromagnetic state undergoes a discontinuous phase transition, while the ferrimagnetic states pass through a continuous phase transition.

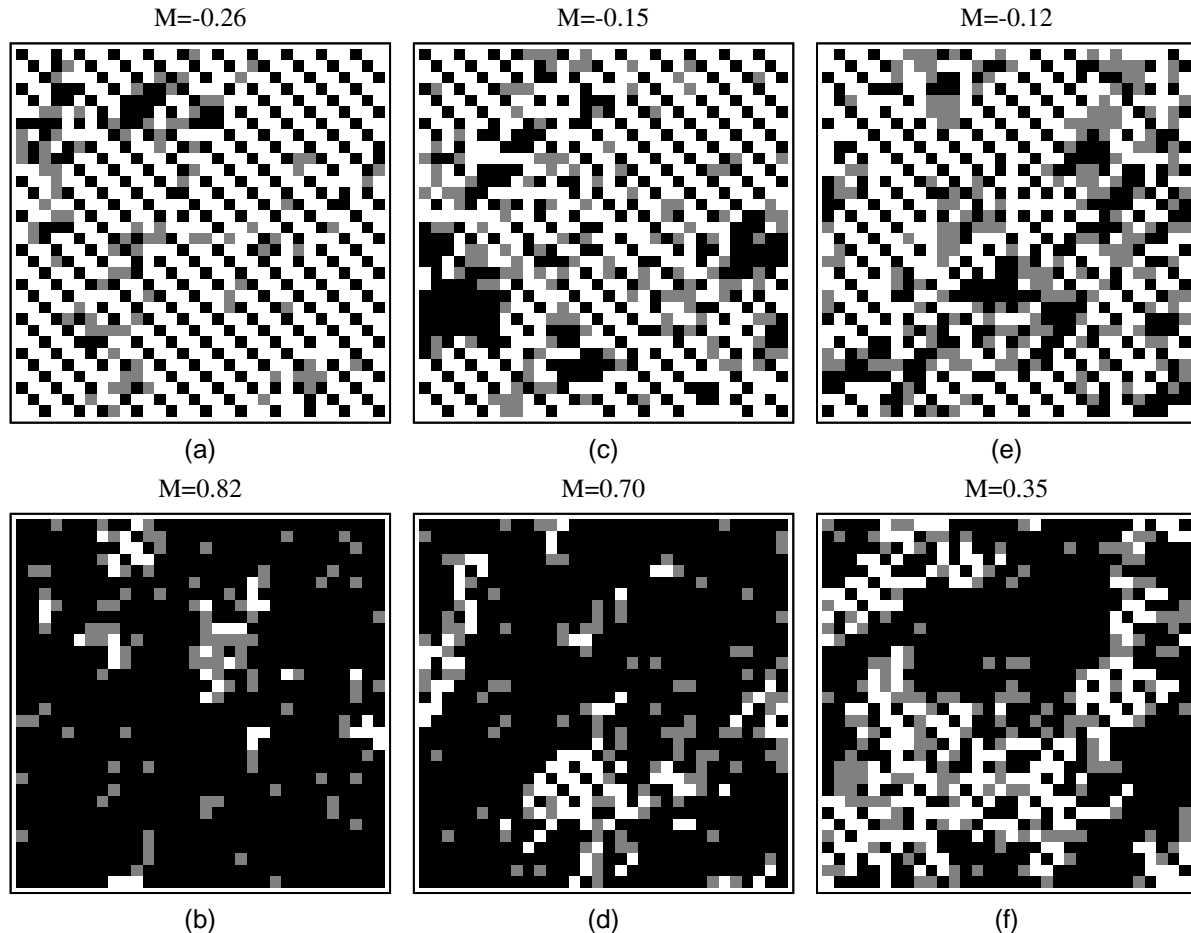


FIG. 17. Configurations corresponding to the peaks of magnetization in the histograms of Fig. 16 (bottom) .

VI. CONCLUSIONS

We studied the spin-1 Baxter-Wu model either considering that it undergoes a continuous, either a discontinuous phase transition. In both cases the results have lead to strong evidences favoring the understanding that the transition is continuous or discontinuous. An analysis of the configurations in the region of the criticality shows the coexistence of ferromagnetic, ferrimagnetic, and paramagnetic agglomerates in different configurations belonging to the criticality, revealing a tetracritical behavior, since the model displays three alternative fer-

rimagnetic constructions. As a result the system may be considered as the zero field multicritical point of possible critical lines of external or crystalline fields.

VII. ACKNOWLEDGEMENTS

We acknowledge the computer resources provided by LCC-UFG and IF-UFMT. L. N. Jorge and L. S. Ferreira acknowledge the support by FAPEG and CAPES, respectively.

-
- [1] L. D. Roelofs, A. Kortan, T. Einstein, and R. L. Park, *Physical Review Letters* **46**, 1465 (1981).
 - [2] P. Piercy and H. Pfnür, *Physical review letters* **59**, 1124 (1987).
 - [3] L. Schwenger, K. Budde, C. Voges, and H. Pfnür, *Physical review letters* **73**, 296 (1994).
 - [4] D. Wood and H. Griffiths, *Journal of Physics C: Solid State Physics* **5**, L253 (1972).
 - [5] R. J. Baxter and F. Wu, *Physical Review Letters* **31**, 1294 (1973).
 - [6] R. Baxter, *Australian Journal of Physics* **27**, 369 (1974).
 - [7] R. Baxter and F. Wu, *Australian Journal of Physics* **27**, 357 (1974).
 - [8] M. Santos and W. Figueiredo, *Physical Review E* **63**, 042101 (2001).

- [9] A. Caparica, S. A. Leão, and C. J. DaSilva, *Physica A: Statistical Mechanics and its Applications* **438**, 447 (2015).
- [10] W. Kinzel, E. Domany, and A. Aharony, *Journal of Physics A: Mathematical and General* **14**, L417 (1981).
- [11] M. L. M. Costa, J. C. Xavier, and J. A. Plascak, *Phys. Rev. B* **69**, 104103 (2004).
- [12] E. K. Riedel, *Phys. Rev. Lett.* **28**, 675 (1972).
- [13] R. B. Griffiths, *Phys. Rev. B* **7**, 545 (1973).
- [14] E. H. Graf, D. M. Lee, and J. D. Reppy, *Phys. Rev. Lett.* **19**, 417 (1967).
- [15] D. P. Landau, B. E. Keen, B. Schneider, and W. P. Wolf, *Phys. Rev. B* **3**, 2310 (1971).
- [16] C. W. Garland and B. B. Weiner, *Phys. Rev. B* **3**, 1634 (1971).
- [17] D. M. Saul, M. Wortis, and D. Stauffer, *Phys. Rev. B* **9**, 4964 (1974).
- [18] G. Musiał, *Phys. Rev. B* **69**, 024407 (2004).
- [19] M. Šimėnas, A. Ibenskas, and E. E. Tornau, *Physical Review E* **90**, 042124 (2014).
- [20] N. G. Fytas, *The European Physical Journal B* **79**, 21 (2011).
- [21] D. A. Dias, J. C. Xavier, and J. A. Plascak, *Phys. Rev. E* **95**, 012103 (2017).
- [22] L. N. Jorge, L. S. Ferreira, S. A. Leão, and A. A. Caparica, *Brazilian Journal of Physics* **46**, 556 (2016).
- [23] M. E. Fisher, *Critical Phenomena*, edited by M. S. Green (Academic Press, 1971).
- [24] M. E. Fisher and M. N. Barber, *Phys. Rev. Lett.* **28**, 1516 (1972).
- [25] A. M. Ferrenberg and D. P. Landau, *Phys. Rev. B* **44**, 5081 (1991).
- [26] A. Caparica, A. Bunker, and D. Landau, *Physical Review B* **62**, 9458 (2000).
- [27] M. S. S. Challa, D. P. Landau, and K. Binder, *Phys. Rev. B* **34**, 1841 (1986).
- [28] K. Binder and D. Heermann, *Monte Carlo simulation in statistical physics: an introduction* (Springer Science & Business Media, 2010).
- [29] K. Vollmayr, J. D. Reger, M. Scheucher, and K. Binder, *Zeitschrift für Physik B Condensed Matter* **91**, 113 (1993).
- [30] K. Binder, *Reports on Progress in Physics* **60**, 487 (1997).
- [31] J. Lee and J. Kosterlitz, *Physical Review B* **43**, 3265 (1991).
- [32] K. Binder and D. P. Landau, *Phys. Rev. B* **30**, 1477 (1984).
- [33] K. Binder, *Reports on progress in physics* **50**, 783 (1987).
- [34] D. P. Landau and K. Binder, *A guide to Monte Carlo simulations in statistical physics* (Cambridge university press, 2014).
- [35] S. Schnabel, D. T. Seaton, D. P. Landau, and M. Bachmann, *Physical Review E* **84**, 011127 (2011).
- [36] F. Wang and D. Landau, *Physical Review E* **64**, 056101 (2001).
- [37] F. Wang and D. Landau, *Physical review letters* **86**, 2050 (2001).
- [38] A. A. Caparica, *Phys. Rev. E* **89**, 043301 (2014).
- [39] A. A. Caparica and A. G. Cunha-Netto, *Phys. Rev. E* **85**, 046702 (2012).
- [40] L. Ferreira and A. Caparica, *International Journal of Modern Physics C* **23**, 1240012 (2012).
- [41] L. S. Ferreira, A. A. Caparica, M. A. Neto, and M. D. Galiceanu, *Journal of Statistical Mechanics: Theory and Experiment* **2012**, P10028 (2012).
- [42] K. W. Post, A. S. McLeod, M. Hepting, M. Bluschke, Y. Wang, G. Cristiani, G. Logvenov, A. Charnukha, G. X. Ni, P. Radhakrishnan, M. Minola, A. Pasupathy, A. V. Boris, E. Benckiser, K. A. Dahmen, E. W. Carlson, B. Keimer, and D. N. Basov, *Nature Physics* (2018), 10.1038/s41567-018-0201-1.